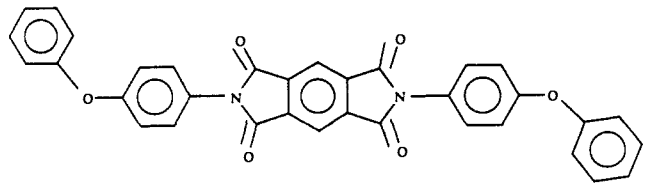

Figure 4. The model compound, MC-IV, investigated to test the convergence of the electronic properties of MC-III.

The nodal plane in the LUMO running along the chain axis and through the imide–phenyl linkage site indicates that the nature of the LUMO in the radical anion will be independent of the nature of the substituent attached to the imide nitrogen.

V. The Converged Electronic Properties of PMDA–ODA PI

An important question that needs to be answered when cluster calculations are performed to estimate the electronic properties of polymers is the following: Did the electronic properties calculated for the polymer of interest from cluster calculations converge?

To answer this question, a full geometry optimization was performed with use of the AM1 and MM2 methods on the neutral form of the model compound MC-IV shown in Figure 4 and AM1 optimizations on the corresponding radical anion. The results of the AM1 computations on the neutral species showed that its IP is 8.91 eV, that is, almost equal to the corresponding one of MC-III, 8.97 eV. In addition, the phenyl–imide torsional angle in the neutral form of MC-IV is 30°, and its remaining minimum energy geometric parameters are almost identical with the corresponding ones in neutral MC-III. The torsional angle between the planes containing the benzene rings in the diphenyl ether moiety is 40°, in good agreement with the X-ray crystal results for substitutionally related compounds that give a value of 45°.[9] The MM2 results were similar to those obtained from AM1.

The LUMO energy of MC-IV is −2.25 eV, that is, identical with the corresponding one in MC-III. Furthermore, its EA was found to be equal to that of MC-III, −2.9 eV. As mentioned above, AM1 tends to overestimate the stability of anions by 10–20 kcal/mol. Therefore, the EA of MC-IV is thus ca. −2 eV. Accordingly, the E_g is also similar to that of MC-III, ~7 eV.

In summary, increasing the size of the model compound did not have any significant effect on the magnitudes of the electronic properties computed for MC-III. This is an indication that the latter properties have converged. Accordingly, the computed electronic properties of MC-III provide reliable estimates of the corresponding ones in PI.

VI. Synopsis

The minimum energy conformation for several PMDA–ODA PI model compounds has been determined via molecular mechanics (MM2) and quantum chemical AM1 computations. The phenyl–imide torsional angle was found to be 30°. Computations on both the neutral and radical anion model compounds provided quantitative determination of the energy gap (7 eV), electron affinity (−2 eV), and ionization potential (8.97 eV). In addition, the barrier to intrachain electron hopping was estimated at 3.2 eV. Finally, qualitative molecular orbital theory was used to aid in the understanding of the electronic and molecular structure of this polymer in a simple orbital interaction context.

Acknowledgment. Dr. S.A. Kafafi acknowledges the financial support of the A. Mellon Foundation and the junior faculty award JHU-BRSG Grant No. H.19.6189, the Johns Hopkins University School of Public Health Computing Center for the allocated cpu-time on the IBM 4381, and the National Institute of Standards and Technology Scientific Computing Division for the donated cpu-time on the ETA-10 supercomputer.

Registry No. (PMDA)(ODA)PI (copolymer), 25038-81-7; MC-III, 14027-98-6; MC-III$^-$, 129731-77-7; MC-IV, 51601-64-0; MC-III (SRU), 25036-53-7.

Methane Formation during Ethylene Decomposition on (1×1)Pt(110)

E. Yagasaki and R. I. Masel*

Contribution from the School of Chemical Sciences, University of Illinois, 1209 West California Street, Urbana, Illinois 61801. *Received May 19, 1989. Revised Manuscript Received October 10, 1989*

Abstract: Previous work on the decomposition of ethylene on a variety of single-crystal surfaces and inorganic clusters indicates that the carbon–carbon bond usually stays intact until after the ethylene is largely dehydrogenated. However, in this paper we find that when ethylene adsorbs on (1×1)Pt(110), the carbon–carbon bond breaks near room temperature yielding methane. The methane desorbs in two peaks centered at 250 and 320 K. There also is evidence for production of a species containing CH_3 groups between 220 and 250 K. By comparison no significant production of methane has been observed during ethylene decomposition on any face of any transition metal studied previously. No methane formation is observed during ethylene decomposition on (2×1)Pt(110) even though all of the sites present on (1×1)Pt(110) are also present on (2×1)Pt(110). This kind of remarkable structure sensitivity has not been observed previously. We propose a speculative mechanism to explain these results involving some special steric hindrances on the (2×1)Pt(110) surface.

Introduction

Over the last 15 years, there have been over a hundred papers which examined ethylene adsorption on various transition-metal surfaces and cluster compounds.[1,2] Generally, the ethylene adsorbs molecularly and then dehydrogenates. There are a few examples where the carbon–carbon bond scission occurs at moderate temperatures.[3-5] There also has been one example where a tiny

(1) Sheppard, N. *Annu. Rev. Phys. Chem.* **1988**, *39*, 589.
(2) Bradley, J. S.; Moskovits, M., Eds. *Metal Clusters*; John Wiley: New York, 1988.
(3) Brucker, C.; Rhodin, T. *J. Catal.* **1977**, *47*, 214.
(4) Lehwald, S.; Erley, W.; Ibach, H.; Wagner, W. *Chem. Phys. Lett.* **1979**, *62*, 360.
(5) Barteau, M. A.; Broughton, J. Q.; Menzel, D. *Appl. Surf. Sci.* **1984**, *19*, 92.

0002-7863/90/1512-8746$02.50/0

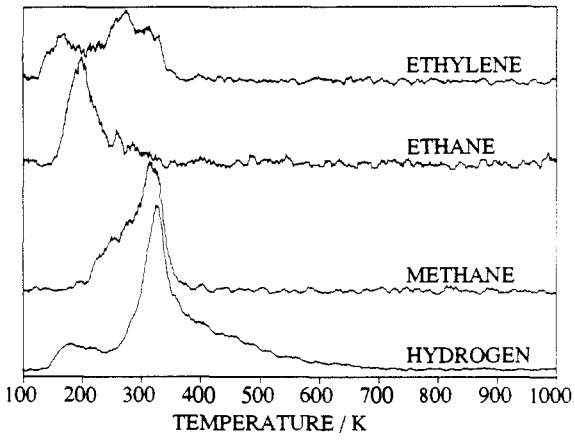

Figure 1. A composite TPD spectrum taken by exposing a clean (1×1)Pt(110) sample to 1×10^{15} molecules/cm^2 of ethylene and then heating at 14 deg K/s. The peak heights have been adjusted to correct for the relative sensitivities of our mass spectrometer.

amount of methane formation was observed during ethylene decomposition on a metal film.[6] However, so far, no one has reported significant production of methane during ethylene decomposition on any transition metal.

Recently, we were examining ethylene decomposition on the (1×1) and (2×1) reconstructions of Pt(110) and were surprised to find that on the (1×1) reconstruction there was significant methane production during the ethylene decomposition process. The methane formation disappeared when we annealed the surface to convert it to a (2×1) reconstruction prior to our admitting the ethylene. In this paper, we will summarize those observations. We will also provide an overview of some EELS measurements which were done to examine the mechanism of the ethylene decomposition on the (1×1)Pt(110) surface.

Experimental Section

The experiments reported in this paper were done using the apparatus and procedures described previously.[7-9] The Pt(110) single-crystal sample used for our previous study[9] of ethylene adsorption on (2×1)Pt(110) was oxidized, sputtered, and annealed until no impurities could be detected by AES and a sharp (2×1) LEED pattern was seen. The sample was then converted to a (1×1) reconstruction via a procedure similar to that of Ferrer et al.[10] The sample was heated to 600 K and exposed to 1×10^{-7} Torr of CO and then slowly cooled to 250 K in 1×10^{-7} Torr of CO. This procedure produced a CO-covered Pt(110) sample with a well-developed (2×1)p1g1 LEED structure and relatively high intensity between the LEED spots. The CO was then pumped away and the sample was cooled to 90 K. The sample was then bombarded for 3 min with 100-V electrons at an average current of 3 mA/cm^2 at 90–240 K to desorb the CO remaining on the surface. A trace of carbon was left behind at the end of the electron bombardment process. This carbon was removed by exposing the sample to 1×10^{-7} Torr of hydrogen at 265 K for 4 min. Then the hydrogen was removed by bombarding the surface with electrons for another 45 s at 90–170 K. At the end of this treatment, the sample showed a sharp (1×1) LEED pattern with little intensity between the spots. The sample also appeared clean by AES. However, TPD and EELS revealed that there was still a small amount of residual CO, H_2, and adsorbed carbon on the surface.

There was concern that these residual impurities were contributing to the unusual chemistry described below. Therefore, we did some experiments where we annealed the surface to 400 or 500 K, to partially convert the sample to a (2×1) reconstruction, and found that the new chemistry we report below could no longer be seen even though the traces of residual impurities could still be seen on the surface.

Once the sample was prepared, it was exposed to a measured amount of ethylene through a capillary array doser. Subsequently, the surface was examined with TPD, EELS, and LEED. One should refer to our previous work[7-9] for details of our procedures for TPD, EELS, and LEED.

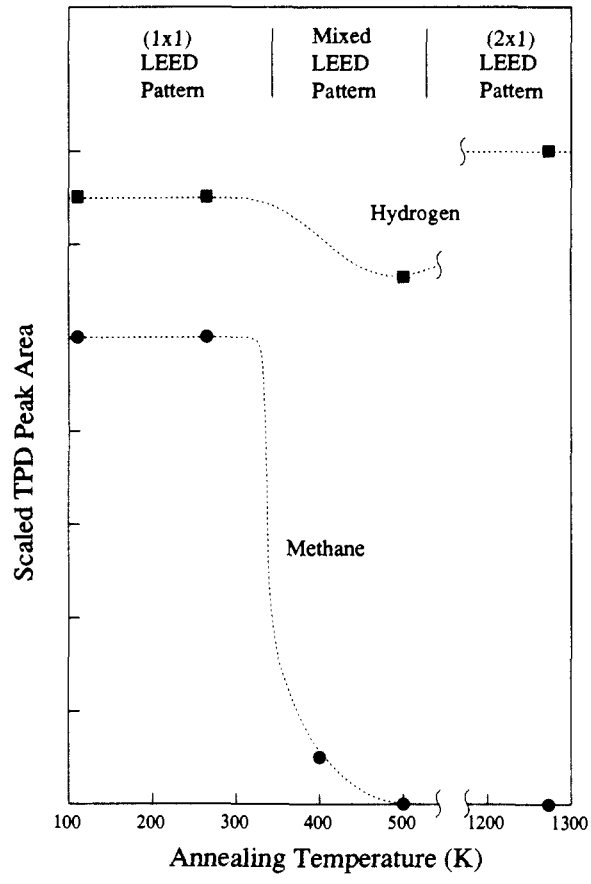

Figure 2. The area of the ethylene and hydrogen peaks measured by preparing a (1×1)Pt(110) surface as described in the Experimental section, annealing to the temperatures indicated, cooling to 93 K, exposing the sample to 1×10^{15} molecules/ cm^2 of ethylene, and then heating at 14 deg K/s. The hydrogen peak areas have been scaled to account for the relative sensitivities of our detection system for hydrogen and methane.

Results

Figure 1 shows a composite TPD spectrum taken by exposing a clean (1×1)Pt(110) sample to 1×10^{15} molecules/cm^2 of ethylene and then heating at 14 deg K/s. Four desorption products were detected during ethylene decomposition on (1×1)Pt(110): ethylene (27 amu), ethane (30 amu), hydrogen (2 amu), and a fraction with peaks at 15 and 16 amu. The ratio of the 15 and 16 amu peaks is as expected for methane desorption and there are no corresponding peaks at 17, 27, 28, or 30 amu. Therefore we attribute the 15 and 16 amu peaks to the desorption of methane which is produced during the ethylene decomposition process. Integration of the peak areas and correcting for the relative sensitivities of our mass spectrometer and relative pumping speeds indicates that the ethylene, methane, and hydrogen desorb in the ratio 1:1.2:2.5. There was some variation in the amount of ethane that desorbed, which we associate with variations in the amount of background hydrogen in the system.

We have also done experiments where we coadsorbed ethylene and hydrogen or ethylene and deuterium on the (1×1)Pt(110) surface. We find that the methane peak shifts to lower temperatures as we add surface hydrogen; the methane peak is at 230 K, when we adsorb 10 L of hydrogen followed by 1 L of ethylene. Such a result suggests but does not prove that the methane forms via a reaction involving surface hydrogen.

We have found that the area of the methane signal is strongly attenuated when the sample is annealed to partially convert it to the (2×1) reconstruction prior to admission of ethylene. Figure 2 shows a plot of the methane and hydrogen peak area as a function of annealing temperature. We find that at temperatures

(6) Wedler, G.; Brenk, M. *Z. Phys. Chem.* **1980**, *119*, 225.
(7) Hatzikos, G. H.; Masel, R. I. *Surf. Sci.* **1987**, *185*, 479.
(8) Lee, F.; Backman, A. L.; Lin, R.; Gow, T. R.; Masel, R. I. *Surf. Sci.* **1989**, *216*.
(9) Yagasaki, E.; Backman, A. L.; Masel, R. I. *J. Phys. Chem.* **1990**, *94*, 1066.
(10) Ferrer, S.; Bonzel, H. P. *Surf. Sci.* **1982**, *119*, 234.

Table I. A Comparison of the Vibrational Frequencies of Ethylene Adsorbed on Pt(110) and Annealed to Various Temperatures to Vibrational Frequencies Observed Previously[a]

tentative assignment	C_2H_4 on (1×1)Pt(110) at 93 K	at 160 K	at 220 K	at 310 K	di-σ C_2H_4 on Pt(111)[13]	Zeise's salt[12]	ethan-1-yl-2-yljdyne on (2×1)Pt(110)[9]	ethylidyne on Pt(111)[13,16,17]	vinylidene on (1×1)Pt(100)[7]
M–C stretch	410	410, 470	410, 500	400, 480	470, 560	369	460	430, 600	452
CH_2, CH_3 rock	670	670	670	700	660	721	670	900	815
CH_2 twist	810 (w)	810	810	800	790		830		
CH_2 wag	950	950	950	1000	980 (sh)	975	990		1048
ν(C–C)	1210	1030, 1210	1030, 1210	1130	1050	1243	1130	1130	1586
CH_3 bend			1350					1350	
CH_2 scissors	1400, 1560	1430, 1560	1430, 1560	1420	1430	1426, 1515	1420		1420
CH_2 stretch	2960, 3060	2960, 3060	2960, 3060	2950	2920	3013, 3079	2920	2950, 2890 (sh)	2920

tentative assignment	C_2D_4 on (1×1)Pt(110) at 93 K	at 220 K	at 310 K	di-σ C_2D_4 on Pt(111)[13]	d_4 Zeise's salt[12]	d_2-ethan-1-yl-2-yljdyne on (2×1)Pt(110)[9]	d_3-ethylidyne on Pt(111)[14]	d_2-vinylidene on (1×1)Pt(100)[7]
M–C stretch	430	430, 480	400	450		430	410	427
CD_2, CD_3 rock			530		525	550	790	
CD_2 twist	590 (w)		680	600		670		
CD_2 wag	709	712	800	740	757	780		709
ν(C–C)	1330	1330	1150	900	1353	1150	1160	1583
CD_3 bend		1145					990	
CD_2 scissors	966	966	1030	1150	1059, 962	1020		1130
CD_2 stretch	2225, 2300	2130, 2225, 2300	2203	2150, 2250	2193, 2331	2208	2080, 2220	2218

[a] Our interpretation of the data is that at 93 K the ethylene mainly adsorbs into a π-bound state with σπ bonding similar to that in Zeise's salt. Some of the π-bound ethylene is converted to a di-π complex upon heating to 160 K. At 220 K we observe the appearance of a 1350-cm^{-1} mode characteristic of the umbrella modes in CH_3 groups. However, no new carbon–carbon bands are detected. Upon further heating the adsorbed ethylene dissociates to yield ethan-1-yl-2-ylidyne ($Pt_3{\equiv}CCH_2Pt$) and hydrogen. w = weak; sh = shoulder.

up to about 265 K, where the (1×1) LEED pattern remains sharp, no changes are seen in the TPD peaks. However, upon annealing to 400–1273 K, the methane peak is substantially attenuated. There also are smaller changes in the hydrogen signal, which we attribute to variations in the background hydrogen levels during the runs.

LEED measurements were also done during the annealing process. The sample still shows a sharp (1×1) LEED pattern after annealing to 265 K. However, by 400 K weak half-order spots appears, suggesting that the surface reconstruction has begun. Half-order spots are clearly visible upon annealing to 500 K. The spots are not sharp yet, so the surface is not fully reconstructed. However, the (2×1) structure is clearly evident. A sharp (2×1) LEED pattern is seen upon annealing to 1273 K.

Notice that there is a close correlation between the changes in the LEED pattern and the changes in the methane desorption signal. The methane signal is large when a (1×1) LEED pattern is observed, while it is strongly attenuated as the (2×1) spots appear. From our data, it appears that the methane peak from a sample which was converted to a (2×1) reconstruction is more than a factor of 100 times smaller than that from the (1×1) reconstruction. As a result we conclude that the methane forms much more readily on the (1×1) reconstruction of Pt(110) than on the (2×1) reconstruction of the same surface.

In our previous work,[7,9] we have also looked for methane formation using the apparatus and procedures identical with those used here. We do not detect methane formation during ethylene decomposition on (1×1)Pt(100), (5×20)Pt(100), or (2×1)Pt(110). There may be a tiny methane peak during ethylene decomposition on Pt(210). However, the methane peak is at least a factor of 50 smaller than the one on (1×1)Pt(110).

We have also examined the decomposition of ethylene on (1×1)Pt(110) with EELS. The results will be discussed in detail in another paper.[11] However, Table I summarizes our findings. We find that when we adsorb ethylene onto a 93 K (1×1)Pt(110) surface, the adsorbed ethylene has an EELS spectrum with peaks in close agreement with the peaks in Hiraishi's IR spectrum of Zeise's salt.[12] Zeise's salt is a prototype of type 2 π-bound ethylene.[1] Therefore, we propose that the ethylene is mainly π-bound on (1×1)Pt(110) at 93 K. Upon annealing to 160 K, the 1210- and 3060-cm^{-1} peaks associated with the carbon–carbon and carbon–hydrogen modes in π-bound ethylene are attenuated.

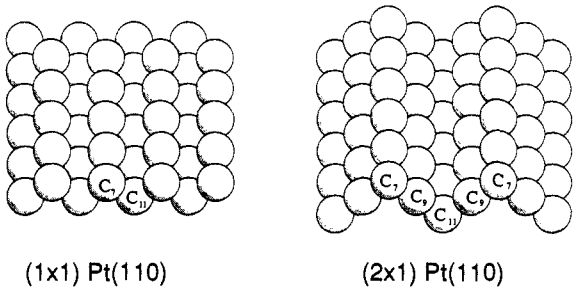

Figure 3. The surface structure of (2×1) and (1×1)Pt(110) as determined by LEED.[10,18]

Simultaneously, a new peak grows into the spectrum at 1030 cm^{-1}, and the peak at 2960 cm^{-1} grows substantially. The new peaks are in positions associated with di-σ-ethylene.[13] Therefore we propose that the π-bound ethylene is partially converted into di-σ-ethylene at 160 K. Upon further heating to 220 K, a new peak appears at 500 cm^{-1}. There is also a shoulder at 1350 cm^{-1}. The 500-cm^{-1} peak does not shift greatly upon deuteration, and it is in a position which Steininger et al.[13] associate with carbon bound in a 3-fold hollow. Therefore we also assign the 500-cm^{-1} peak to carbon in a 3-fold hollow. The 1350-cm^{-1} peak is harder to identify. Steininger et al.[13] show that the methyl groups in adsorbed ethylidyne ($\mu_3{\equiv}CCH_3$) show an umbrella mode at 1350 cm^{-1}. The 1350-cm^{-1} peak in our spectra shifts appropriately with deuteration, and it is about a third as intense as the 1350-cm^{-1} mode in our previous[9] spectrum of ethylidyne on (2×1)Pt(110). We do not observe a mode at 1130 cm^{-1} characteristic of the carbon–carbon mode in ethylidyne. Thus, it is unlikely that unstrained μ_3-ethylidyne forms on (1×1)Pt(110). However, the presence of the 1350-cm^{-1} mode suggests that either a methyl group or some species containing a methyl group forms when ethylene decomposes on (1×1)Pt(110) at 220 K.

The 1350-cm^{-1} mode disappears upon annealing to 310 K. The 310 K EELS spectrum is complicated. However, upon annealing to 330 K, we observe an EELS spectrum which matches one we previously[9] attributed to ethan-1-yl-2-ylidyne.

In a previous paper[9], we have also examined ethylene decomposition on (2×1)Pt(110) with EELS. We observe a mixture of di-σ and π-bound ethylene on (2×1)Pt(110). However, the 500-

(11) Yagasaki, E.; Masel, R. I. *Surf. Sci.* To be published.
(12) Hiraishi, J. *Spectrochim. Acta* **1969**, *25A*, 749.
(13) Steininger, H.; Ibach, H.; Lehwald, S. *Surf. Sci.* **1982**, *117*, 685.

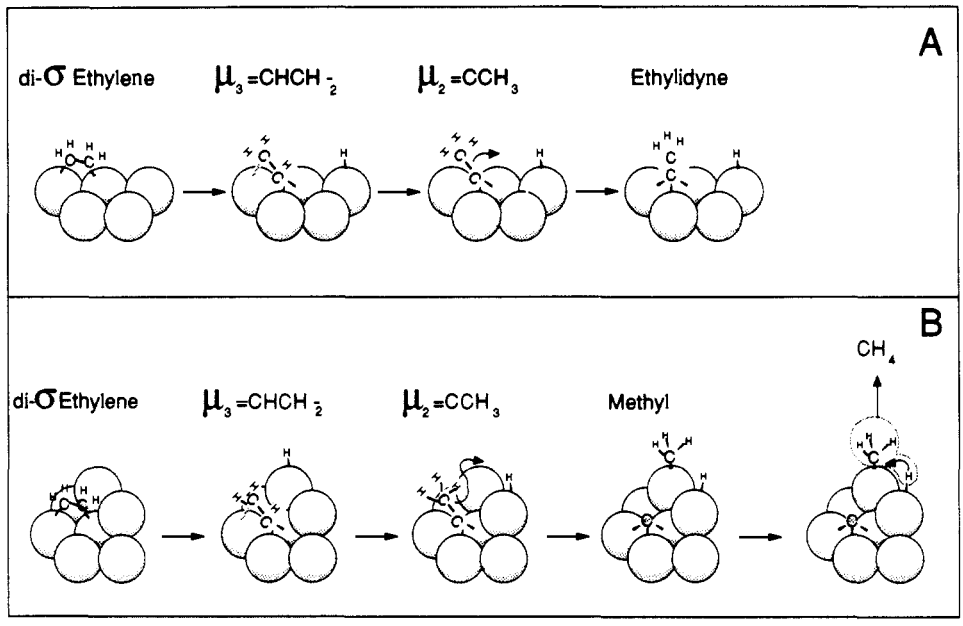

Figure 4. (A) The mechanism of ethylidyne formation on Pt(111) from ref 14. (B) A possible mechanism for methane formation on (1×1)Pt(110).

and 1350-cm^{-1} modes are not observed. Thus, the 500- and 1350-cm^{-1} modes seem to be associated with chemistry which is unique to (1×1)Pt(110).

Discussion

The results here show that ethylene decomposition on (1×1)Pt(110) shows much different characteristics than ethylene decomposition on other faces of platinum. We observe significant methane formation on the (1×1) reconstruction of Pt(110). However, no methane is detected on (2×1)Pt(110), (1×1)Pt(100), or (5×20)Pt(100). Further, when we anneal the (1×1)Pt(110) surface to 400–500 K to partially reconstruct the (1×1)Pt(110) surface to a (2×1) reconstruction, the methane formation is strongly attenuated. In our previous work[9] we found that the carbon–carbon bond remains intact upon heating to at least 400 K on (2×1)Pt(110). Yet here we observe carbon–carbon bond scission below room temperature, as evidenced by the methane formation. Clearly, the (1×1) and (2×1) reconstructions of Pt(110) are showing much different chemistry.

It is rather unexpected that (1×1) and (2×1)Pt(110) behave this differently. Figure 3 shows the structure of these two surfaces. The (1×1)Pt(110) contains C_7 and C_{11} atoms. There are a series of 3-fold hollow sites and bridge sites on the surface. However, all of the sites present on (1×1)Pt(110) are also present on (2×1)Pt(110). The spacing of the steps is different on (1×1) and (2×1)Pt(110) and there are some extra sites on (2×1)Pt(110). However, there are no extra sites on (1×1)Pt(110). The site densities on (1×1)Pt(110) are only twice those on (2×1)Pt(110). In the literature, it is normally assumed that a doubling of step densities will only produce a doubling in rate. Thus, it is truly surprising that (1×1)Pt(110) is more than a factor of 100 more active than (2×1)Pt(110) for carbon–carbon bond scission and resultant methane formation.

At present we do not have detailed mechanistic information which explains why the rate of methane formation is so much higher on (1×1)Pt(110) than on (2×1)Pt(110). However, we do know that the methane peak shifts to lower temperature with increasing hydrogen coverage, and we do see some new peaks in EELS. Therefore, we decided to propose a speculative mechanism to try to explain why (1×1)Pt(110) behaves so much differently than (2×1)Pt(110).

As noted above, we find that at 93 K, the ethylene adsorbs mainly into a type 2 π-bound complex. The π-bound complex partially converts to a di-σ complex upon heating to 160 K. Upon further heating we observe methane formation. The details of the methane formation process are unclear from our data. However, one possibility is that the reaction follows the mechanism

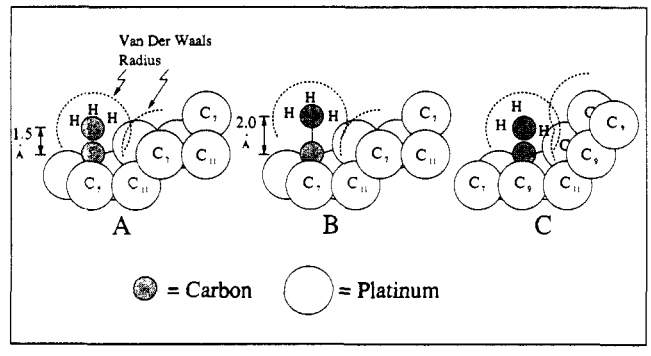

Figure 5. (A) The geometry of an ethylidyne on (1×1)Pt(110) assuming that the ethylidyne forms over a 3-fold FCC hollow and the bond lengths and angles are the same as on Pt(111). Notice that the van der Waals radius of the methyl group overlaps the van der Waals radius of the C_7 platinum atom. (B) A repeat of (A) assuming that the carbon–carbon bond length was expanded by 0.5 Å. Notice that the van der Waals radii no longer overlap. (C) The geometry of an ethylidyne on (2×1)Pt(110) assuming that the ethylidyne forms over a 3-fold FCC hollow and the bond lengths and angles are the same as on Pt(111). Again the van der Waals radii overlap. However, in contrast to case (A) and (B), the overlap increases if the carbon–carbon bond stretches.

in Figure 4B. Zaera has shown that on Pt(111) di-σ ethylene can dehydrogenate over a 3-fold FCC hollow site to form a multiply bound vinyl species. Then there is a 1,2-hydrogen shift to yield ethylidyne.[14] See Figure 4A. There are FCC hollows on (1×1), thus it seems reasonable that the same chemistry which Zaera observes on Pt(111) could start to occur on (1×1)Pt(110). First one would get a vinyl species then a 1,2-hydrogen shift. However, the ethylidyne cannot stand up over the 3-fold FCC hollows on (1×1)Pt(110) since if the ethylidyne were in an upright position the van der Waals radius of the methyl group in the ethylidyne would overlap the van der Waals radius of the platinum atom as shown in Figure 5A. The ethylidyne would fit if the carbon–carbon bond in the ethylidyne stretched by about 0.5 Å as shown in Figure 5B. As a result, steric repulsions between the methyl group and the surface would be reduced as the carbon–carbon bond extends. This would provide a driving force for bond extension on (1×1)Pt(110). If the bond stretches, it might easily break. Thus, the mechanism in Figure 4B provides a possible

(14) Zaera, F. *J. Am. Chem. Soc.* **1989**, *111*, 4240.

pathway for carbon-carbon bond scission on (1×1)Pt(110).

In contrast, however, on (2×1)Pt(110) the methyl group in an upright ethylidyne would overlap both the C_7 and the C_9 atom on the (2×1)Pt(110) surface as shown in Figure 5C. While the overlap with the C_9 atom decreases as the bond extends, the overlap with C_7 atom increases. The increase in the overlap with the C_7 is larger than the decrease in the overlap with the C_9 atom. Consequently, while there is a driving force for bond extension on (1×1)Pt(110), the extra steric hindrances on the (2×1)Pt(110) surface would inhibit carbon-carbon bond scission on (2×1)Pt (110). As a result, the mechanism in Figure 4B explains why bond scission is more likely on (1×1)Pt(110) than on (2×1)Pt(110) as is observed.

If bond scission occurs, one would produce a methyl group. Henderson et al.[15] show that methane formation from recombination of hydrogen and methyl radicals occurs quite readily at 290 K on Pt(111) in the presence of chlorine. Hence, similar chemistry is quite feasible on (1×1)Pt(110).

Admittedly, the mechanism in Figure 4B is speculative. We do not have direct evidence that a deformed ethylidyne actually forms on (1×1)Pt(110). There is a 1350-cm^{-1} stretch in EELS which might be associated with either a deformed ethylidyne or some other species containing a CH_3 group such as an isolated methyl group. However, our evidence for formation of a strained ethylidyne intermediate is not strong. Still, the mechanism in Figure 4B does explain our observations. All of the steps except the carbon-carbon bond scission step have been observed previously on other faces of platinum. A carbon-carbon bond scission process clearly occurs since we observe a methane desorption product. We observe a decrease in the methane desorption temperature as we add surface hydrogen, which is suggestive that the methane forms via a recombination process. However, isotopic exchange experiments to prove this mechanism were inconclusive. Thus, we propose the mechanism in Figure 4B as a tentative, but by no means definitive, explanation of our data.

Conclusions

In summary then, in this paper we present the first clear evidence for methane formation during ethylene decomposition on any single-crystal transition-metal surface. We find that methane formation occurs on a (1×1) reconstruction of Pt(110). However, it is not observed on the (2×1) reconstruction of Pt(110). Yet there are no sites present on (1×1)Pt(110) which are not also present on (2×1)Pt(110). We have proposed that the methane formation occurs by the mechanism in Figure 4B. All of the steps in this mechanism have been observed on other surfaces of platinum. Further, the mechanism in Figure 4B explains our observations, including the unprecedented structure sensitivity of the methane formation reaction. However, our evidence for this mechanism is by no means definitive.

Acknowledgment. This work was supported by the National Science Foundation under Grant CBT 86-13258 and by Amoco Oil Co and Shell USA. Sample preparation was done using the facilities of the University of Illinois Center for Microanalysis of Materials which is supported as a national facility, under National Science Foundation Grant DMR 86-12860. Equipment was provided by NSF Grants CPE 83-51648 and CBT 87-04667.

(15) Henderson, M. A.; Mitchell, G. E.; White, J. M. *Surf. Sci. Lett.* **1987**, *184*, L325.
(16) Kesmodel, L. L.; Dubois, L. H.; Somorjai, G. A. *Chem. Phys. Lett.* **1978**, *56*, 267.
(17) Skinner, P.; Howard, M. W.; Oxton, I. A.; Kettle, S. F. A.; Powell, D. B.; Sheppard, N. *J. Chem. Soc., Faraday Trans. 2* **1981**, *77*, 1203.
(18) Adams, D. L.; Nielsen, H. B.; VanHove, M. A.; Ignatiev, S. *Surf. Sci.* **1987**, *104*, 47.

Determination of the Acidity of Lewis Acids

Pierre Laszlo* and Michelle Teston

Contribution from the Laboratoire de Chimie Fine aux Interfaces Ecole Polytechnique, 91128 Palaiseau Cedex, France. *Received April 24, 1990*

Abstract: The chemical shift (H-3) of crotonaldehyde complexed by a Lewis acid provides a measure of its strength as a catalyst, according to R. F. Childs, D. L. Mulholland, and A. Nixon, (*Can. J. Chem.* **1982**, *60*, 801-808). A theoretical justification was highly desirable and is provided here: the experimental method works because of the linear dependence of the H-3 chemical shift on the energy of the lowest π^* MO in the complex. While the experimental determination has some drawbacks (problems of precise concentration, solubility, impurities, and availability), MO calculations appear trustworthy and have some advantages for the estimation of the catalytic activity of a Lewis acid.

Introduction

Numerous recent studies make use of Lewis acids to catalyze organic reactions. These include, as prime examples, Diels-Alder[1] and [2 + 2][2] cycloadditions, ene reactions,[3] aldol condensations,[1e-4] Michael 1,4-additions,[5] the reaction of acetals with olefins and unsaturated ethers,[6] and Claisen[7] rearrangements, besides other textbook cases such as Friedel-Crafts alkylations and acylations.[8]

(1) (a) Lamy-Schelkens, H.; Gioni, D.; Ghosez, L. *Tetrahedron Lett.* **1989**, *30*, 5887-5890. (b) Maruoka, K.; Yamamoto, H. *J. Am. Chem. Soc.* **1989**, *111*, 789-790. (c) Midland, M. M.; Afonso, M. M. *J. Am. Chem. Soc.* **1989**, *111*, 4368-4371. (d) Narasaka, K.; Iwasawa, N.; Inoue, M.; Yamada, T.; Nakashima, N.; Sugimori, J. *J. Am. Chem. Soc.* **1989**, *111*, 5340-5345. (e) Corey, R.; Imwinkelried, E. J.; Pikul, S.; Xiang, Y. B. *J. Am. Chem. Soc.* **1989**, *111*, 5493-5495.
(2) (a) Doxsee, K. M.; Farahi, J. B. *J. Am. Chem. Soc.* **1988**, *110*, 7239-7240. (b) Trost, B. M.; Yany, B.; Miller, M. L. *J. Am. Chem. Soc.* **1989**, *111*, 6482-6484. (c) Lewis, F. D.; Barancyk, S. V. *J. Am. Chem. Soc.* **1989**, *111*, 8653-8661.
(3) (a) Snider, B. B. *Acc. Chem. Res.* **1980**, *13*, 426-432. (b) Tietze, L. F.; Beifuss, U.; Ruther, M. *J. Org. Chem.* **1989**, *54*, 3120-3129. (c) Mikami, K.; Terada, M.; Nakai, T. *J. Am. Chem. Soc.* **1989**, *111*, 1940-1941.
(4) (a) Ojima, I.; Kwon, H. B. *J. Am. Chem. Soc.* **1988**, *110*, 5617-5621. (b) Danishefsky, S. J.; Simoneau, B. *J. Am. Chem. Soc.* **1989**, *111*, 2599-2604. (c) Hegel, G.; Thornton, E. R. *J. Am. Chem. Soc.* **1989**, *111*, 5722-5728.
(5) (a) Lipshutz, B. H.; Ellsworth, E. L.; Siahaan, T. J. *J. Am. Chem. Soc.* **1988**, *110*, 4834-4835. (b) Lipshutz, B. H.; Ellsworth, E. L.; Siahaan, T. J. *J. Am. Chem. Soc.* **1989**, *111*, 1351-1358. (c) Cabral, J.; Laszlo, P.; Mahé, L.; Montaufier M. T. *Tetrahedron Lett.* **1989**, *30*, 3969-3972.
(6) (a) Povarov, L. S. *Russ. Chem. Rev. (Engl. Transl.)* **1975**, *34*, 639-656. (b) Hoaglin, R. J.; Hirsh, D. H. *J. Am. Chem. Soc.* **1949**, *71*, 3468-3472. (c) Isler, O.; Lindlar, H.; Montavon, M.; Rüegg, R.; Zeller, P. *Helv. Chim. Acta* **1956**, *39*, 249-259. (d) Isler, O.; Montavon, M.; Rüegg, R.; Zeller, P. Swiss Patent 317112, 1956.
(7) (a) Maruoka, K.; Nonoshita, K.; Banno, H.; Yamamoto, H. *J. Am. Chem. Soc.* **1988**, *110*, 7922-7924. (b) Nonoshita, K.; Banno, H.; Maruoka, K.; Yamamoto, H. *J. Am. Chem. Soc.* **1990**, *112*, 316-322.

0002-7863/90/1512-8750$02.50/0